Anion···Anion Interactions Involving σ-Holes of Perrhenate, Pertechnetate and Permanganate Anions

Andrea Daolio,[a] Andrea Pizzi,[a] Giancarlo Terraneo,[a] Antonio Frontera,[b] and Giuseppe Resnati*[a]

Dedicated to Professor Renato Ugo, in memory of his unforgettable scientific and human qualities

In this communication experimental and theoretical results are reported affording strong evidence that interactions between electron rich atoms and the metal of tetroxide anions of group 7 elements are a new case of attractive and σ-hole interactions. Single crystal X-ray analyses, molecular electrostatic potentials, quantum theory of atoms-in-molecules, and noncovalent interaction plot analyses show that in crystalline permanganate and perrhenate salts the metal in Mn/ReO_4^- anion can act as electron acceptors, the oxygen of another Mn/ReO_4^- anion can act as the donor and supramolecular anionic dimers or polymers are formed. The name matere bond (MaB) is proposed to categorize these noncovalent interactions and to differentiate them from the classical metal-ligand coordination bond.

The electron density at the outer regions of covalently bonded atoms is higher in some zones and lower in some others. The electrostatic potential tends to be negative, or less positive, in former regions and positive, or less negative, in the latter. For instance, a region of depleted electron density (σ-hole) is typically present on the extension of a σ covalent bond and opposite to the atom.[1] The electrostatic potential at the σ-hole can be remarkably positive if it is opposite to a strong electron withdrawing group.[2,3] Regions of depleted electron density and quite positive electrostatic potential can be present also above and below a flat area in a molecular entity (π-holes).[4–6] Molecular regions where the electrostatic potential is positive (electrophilic sites) tend to attractively interact with regions of negative potential (nucleophilic sites) in the same or nearby molecules. This tendency, in synergy with other phenomena, *e.g.*, polarization, dispersion, and charge transfer, determines the formation of intra- and intermolecular interactions.

This mindset for rationalizing interactions was first proposed[7] and used[8] for monovalent halogens acting as electrophiles and it rapidly developed into a systematic categorization of interactions wherein the electrophile is an element of any group of the p block.[2,3,9–12] In 2014 we observed[13] that the same mindset can be used for rationalizing some interactions formed by elements of the d block. The presence of σ- and π-holes in derivatives of elements of groups 8,[14] 11,[15] and 12[16] has been subsequently reported. The role of these holes in the formation of attractive interactions has been identified and used to rationalize the interactional landscape in a variety of systems.

Here we report how the same mindset allows for rationalizing some counterintuitive interactions formed by derivatives of group 7 elements. Specifically, experimental and theoretical evidences are described proving that perrhenate, pertechnetate and permanganate anions possess, at the metal, regions of depleted electron density which are involved in the formation of short and directional contacts[17] with electron donor sites. Single crystal X-ray analyses of melaminium perrhenate (2,4,6-triamino-1,3,5-triazin-1-ium perrhenate, **1a**) and permanganate (**1b**) show the presence of anion···anion interactions wherein the oxygen of one unit gets close to the transition metal of another unit approximately on the extension of a Mn/Re–O covalent bond and affords infinite chains and dimeric adducts, respectively (Figure 1). The electron donor site approaching the transition metal can also be a neutral lone pair possessing atom as it is the case for the carboxylic oxygen in betaine perrhenate (1-carboxy-*N*,*N*,*N*-trimethylmethanaminium perrhenate, **2**). Molecular electrostatic potential (MEP) surface calculations of the anions and their ammonium salts suggest that these short and linear O–Mn/Re···O contacts can be rationalized as σ-hole interactions. The quantum theory of "atoms-in-molecules" (QTAIM) combined with the noncovalent interaction plot (NCIplot) index analyses prove the existence and attractive nature of Mn/Re···O contacts in the solid.

A categorization of σ- and π-hole interactions refers to the group, in the periodic table, of the atom at the electrophilic site.[13,19] The resulting taxonomy of interactions is highly

[a] *A. Daolio, Dr. A. Pizzi, Prof. Dr. G. Terraneo, Prof. Dr. G. Resnati*
Department of Chemistry, Materials and Chemical Engineering "Giulio Natta"
Politecnico di Milano
via Mancinelli 7, 20131 Milano, Italy
E-mail: giuseppe.resnati@polimi.it
[b] *Prof. Dr. A. Frontera*
Department of Chemistry
Universitat de les Illes Balears
Crta. de Valldemossa, 07122 Palma de Mallorca (Baleares), Spain

Supporting information for this article is available on the WWW under https://doi.org/10.1002/cphc.2021006817

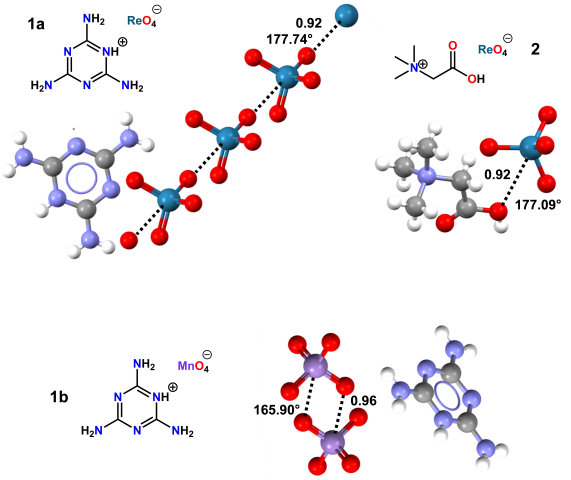

Figure 1. Ball and stick representation of the supramolecular polyanionic chain, dimer and cation-anion pair assembled by MaB in crystals of **1a** (top left), **1b** (bottom) and **2** (top right). For sake of clarity, structural formulas of the salts are reported and only one cation is depicted per structure. The normalized contacts (Nc)[18] and O–Mn/Re···O angles are given close to the MaB. Color code: whitish, hydrogen; grey, carbon; red, oxygen; blue, nitrogen; bluish, rhenium; violet, manganese.

descriptive as the electrophilic site in the interaction is unequivocally identified and information is conveyed on specific features of the subset of σ/π-hole bonding the interaction belongs to. For instance, by naming a σ/π-hole interaction halogen bond[2] or tetrel[9] bond, it is communicated that a small deviation from linearity is expected (as this is typical for group 17 and 14 elements) and by naming an interaction chalcogen bond[1,3] or pnictogen bond,[1,10] the message is given that probable deviation is slightly or consistently greater than the two cases above (as characteristic for group 16 and 15 elements, respectively). The categorization sketched above offers the additional advantages of being comprehensive (it gives consistent names to a wide set of interactions involving many elements) and systematic (it refers to the group to which the electrophilic atom belongs). Finally, it avoids an excessive sprawling of terms, as it would be the case if interactions would be identified by referring to the name of the electrophilic element. No trivial name is available for group 7 elements and the term matere bond (MaB, Ma = Mn, Tc, Re, (Bh)) is proposed to designate interactions described in this paper and other interactions wherein a group 7 element is the electrophile. Matere is the acronym obtained unifying the first two letters of the name of best known group 7 elements.

MnO_4^- anion is a strong oxidizer used in redox quantitative analyses and TcO_4^- is commonly used in nuclear medicine. ReO_4^- anion is non-oxidizing, its chemistry is similar to that of TcO_4^- and is used in radiodiagnostic procedures as a carrier for trace levels of TcO_4^-. Crystals of melaminium and betaine perrhenate or permanganate **1a**, **2a**, and **1b** were obtained through salt methatesis reaction between respective hydrochlorides and $AgReO_4$ or $KMnO_4$ (Section S2). Single crystal X-ray analyses of these salts revealed the details of the interactional landscape in the solid (Section S3). The crystal packings are characterized by tight networks of hydrogen bonds (HBs). In **1a**,**b** the melaminium units are assembled into infinite ribbons[20] by two HBs and additional HBs append the perrhenate and permanganate units to the ribbons (Figures S4 in the Supporting Information). In **2a**, eleven of the twelve hydrogen atoms of betaine cation form HBs and any betaine unit is hydrogen bonded to five perrhenate anions and four other betaines (Figure S5). Notwithstanding the severe geometric constrains resulting from these tight HBs networks and the electrostatic cation-anion attraction, probably the strongest attractive force in the three salts, short and linear O–Mn/Re···O contacts are present in all three systems.

In **2**, the hydroxyl oxygen of betaine gets close to rhenium. The geometry of the interaction is consistent with the involvement of one of the oxygen lone pairs in a σ-hole bonding as the C–O···Re angle is 113.45° and the O–Re···O angle is 177.09°. In **1a** and **1b** the nucleophile is the oxygen of another anionic unit and the Mn/Re···O MaBs form quite linear polyanionic infinite chains in **1a** (the O–Re···O angle is 177.74°) and parallelepiped shaped dimers in **1b**. Both binding motifs are found in other σ-hole bonded systems, *e.g.*, in spodium,[21] pnictogen,[10,22] and chalcogen[3,23] bonded structures. The observed Mn/Re···O separations are well below the sum of van der Waals radii of involved atoms, normalized contacts (Nc)[18] spanning the range 0.92–0.96. The Re···O contacts are shorter and more directional than the Mn···O contact, consistent with typical tendencies of σ-hole interactions. In fact, when different elements of the same group of the periodic table are σ-hole bonded to a given nucleophile, the heavier elements afford shorter and more directional interactions than the lighter elements.[2,10–12]

An analysis of the Cambridge Structural Database (CSD) indicates that the tendency of perrhenate anion to form short and directional Re···O MaB is quite general (Table S19, S20). A Re···O MaB is present in ~19% of structures containing a ReO_4^- anion and in most cases (~75% of the matere bonded systems) the MaB is an anion···anion interaction involving ReO_4^- units. The directional preference of these contacts is that typical for σ-hole interactions (Figure 2). Occasionally, the nucleophilic atom

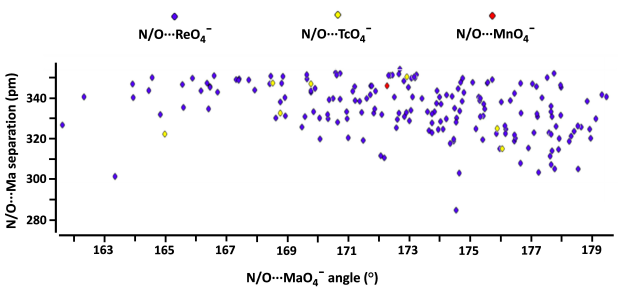

Figure 2. Scatterplot of Ma···O/N separations *vs.* O–Ma···O/N angles in MaO_4^-···O/N MaBs present in CSD structures (Tables S19–S23).

forming the MaB with the ReO_4^- anion is a lone pair possessing atom different from oxygen, e.g., a nitrogen or chlorine atom, either neutral or anionic (Table S21).

In the CSD also structures wherein TcO_4^- and MnO_4^- anions form matere bonded anion···anion adducts are present (Tables S22, S23). While the numbers of structures containing these two anions are too small to allow for precise generalizations to be made, it can be dependably stated that TcO_4^- and even more MnO_4^- anions are less prone to form MaBs than ReO_4^-. This is consistent with the general tendency of the heavier elements of a given group of the periodic table to act as better electrophiles (namely to form more frequently the corresponding σ-hole interactions) than the lighter elements of the same group.

Theoretical studies have been carried out to assess the existence and attractive nature of O–Mn/Re···O contacts. The MEP surfaces of the MaO_4^- anions and their ammonium salts (used as minimalistic models of the cations of **1 a**,**b** and **2**) were calculated first (Figure 3). As expected, the MEP values of the isolated anions are negative in the entire surface due to their net negative charge. Four negative σ-holes (regions where the MEP values are less negative) are present at the extensions of the four O–Ma bonds. The MEP values at the σ-holes become less negative on moving down in the group, as typical in σ-hole interactions. The MEP difference at the σ-holes is significant moving from Mn to Tc ($+24$ kcal mol^{-1}) and is minor from Tc to Re ($+3$ kcal mol^{-1}). However, the σ-hole is larger at Re than at Tc. It is worth highlighting that the MEP value at the σ-holes of the $[NH_4][MaO_4]$ salts remains negative for the Mn salt, but reduced to -8.7 kcal mol^{-1}, while becomes positive for the heavier Tc and Re elements, thus suitable to attractively interact with atoms with negative potential.

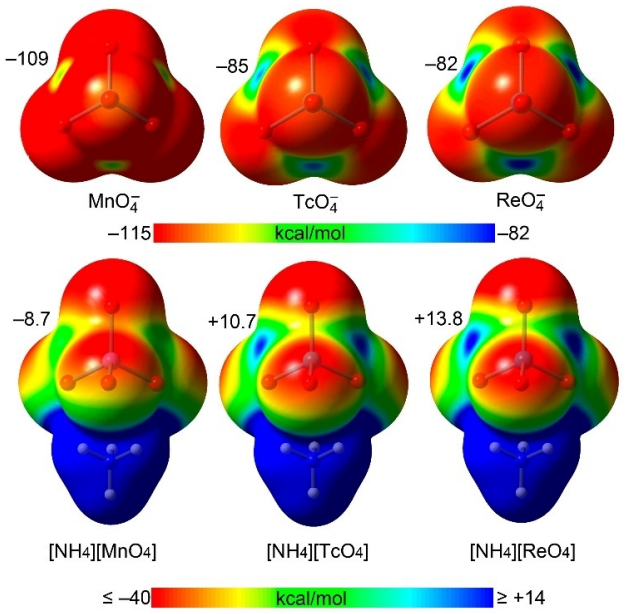

Figure 3. MEP surfaces of MaO_4^- (Ma = Mn, Tc and Re) anions and their ammonium salts at the PBE0-D3/def2-TZVP level of theory. The values at σ-holes are given in kcal mol^{-1}.

The Mn/Re···O contacts in **1 a**,**b** and **2** were further characterized by using the QTAIM and the NCIPlot. The analyses of representative ternary assemblies extracted from the X-ray structures are depicted in Figure 4. The respective formation energies (calculated from the three isolated ions) are large and negative due to the strong attraction between the counterions. The QTAIM analysis nicely confirms the existence of the Re···O contact in **1 a**, that is characterized by a bond critical point (CP) and bond path connecting the Re atom to the O atom. The analysis also reveals the existence of two N–H···O HBs between the melaminium cation and the anion, evidenced by the corresponding bond CPs and bond paths (Figure 4). Finally, the analysis shows the existence of anion–π interactions, characterized by several bond CPs and bond paths connecting the perrhenate anion to the melaminium cation. The existence of the MaB interaction is also confirmed by the NCIplot analysis that shows a green isosurface (attractive interaction) located between the Re and O atoms. In compounds **1 b** and **2**, the QTAIM analysis shows that a bond CP and a bond path do not connect the O-atom of an anion to the Ma atom of an adjacent anion, instead to an O atom of the adjacent anion. For **1 b** this is likely due to the poorer

directionality of the MaB compared to **1 a**. A similar behaviour has been described in osme bonds involving $O_3Os{=}N\text{-}R$ compounds.[14] For **2**, where the MaB directionality is similar to that in **1 a**, the deviation of the bond path toward the closest O atom can be related to the orientation of a lone pair belonging to the electron donor O atom. Therefore, in compounds **1 b** and **2**, the interaction is only revealed by the

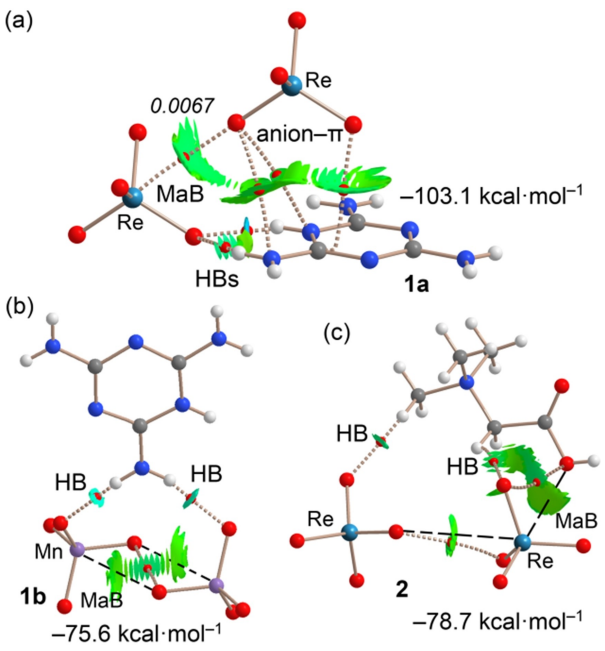

Figure 4. QTAIM distribution of intermolecular bond critical points (red spheres) and bond paths for the trimeric assemblies of compounds **1 a** (a), **1 b** (b) and **2** (c). The electron density at the bond CP that characterizes the MaB is given in italics (a.u.) The superimposed NCIplot isosurface (RDG isovalue = 0.5 a.u.) is shown, the cut-off ρ = 0.04 a.u. has been used. Color range -0.035 a.u. $\leq (\text{sign}\lambda_2)\,\rho \leq 0.035$. Level of theory: PBE0-D3/def2-TZVP.

NCIplot index analysis. In fact, the size of the NCI surface is larger for the Ma···O than for the O···O contact. In the ternary assemblies of compounds **1 b** and **2**, the QTAIM analysis also evidences the existence of additional C/N–H···O HBs that further contribute to the stabilization of the assemblies.

We have also studied if orbital contributions are important in the Mn/Re···O interactions described above. For this purpose, the natural bond orbital (NBO) second order perturbation analysis has been done since it is convenient to reveal donor-acceptor interactions.[24] Indeed, the calculations show modest orbital contributions in all complexes. They come from electron donations from the lone pair (LP) at the oxygen atom to the antibonding Re/Mn–O bonds thus supporting the σ-hole nature of the interaction where the Re/Mn atom is acting as acceptor and the O atom as donor of electron density. The $E^{(2)}$ values are 3.22, 0.31 and 2.72 kcal mol^{-1} for **1 a**, **1 b** and **2**, respectively, evidencing that the heavier Re element presents stronger orbital effects, in line with the shorter experimental distances.

In order to assess the generality of the formation of ReO_4^-···ReO_4^- MaBs, we computed the energy profile (interaction energy *vs* distance, Figure 5) for the ReO_4^-···ReO_4^- dimer in gas phase and in solution. The dimer (in the absence of counterions) is obviously not stable in the gas phase and the monomers separate to infinitum (inset graph in Figure 5). In solid **1 a**, the $(\cdots ReO_4^-)_n$ polymer feels the influence of the surrounding molecules. We have modelled this effect by computing the dimer using a continuum solvation model and the dielectric constants of two different solvents (DMSO and water). Gratifyingly, we have observed that the ReO_4^-···ReO_4^- dimer is energetically favorable in water (Figure 5, blue line) as two separate monomers are less stable than the dimer by 0.6 kcal mol^{-1}. In DMSO (red line) the interaction energy of the dimer is negligible and a local minimum around d ≈ 4 Å is found with a small barrier (0.8 kcal/mol). These results suggest that the electrostatic repulsion of anion···anion MaBs can be balanced by a convenient environment and the interactions may exist in solution even without the counterion participation. Although the dielectric constant of any crystalline compound is not known, it can be expected that the stabilization of the ReO_4^-···ReO_4^- adduct is higher in the ionic environment of crystalline salts than in solution.

Finally, the three MaO_4^- dimers (Ma = Mn, Tc and Re) have been further investigated taking into consideration solvent effects (water). Results of QTAIM/NCIplot analyses of the three dimers are given in Figure 6 where the dimerization energies and Ma···O distances are reported. Since the interaction energies are very small (smaller than the accuracy of the PBE0-D3 functional), they have been computed using also the gold standard CCSD(T) *ab initio* method. Very similar results (in italics in Figure 6) were obtained and the reliability of the used DFT functional is validated. The QTAIM analysis shows the existence of a bond CP and bond path connecting the Ma atom to the O atom in the three homodimers. The interaction is further characterized by a NCIplot green isosurface. Due to the large effect of water, differences in the interaction energies are very small. The interaction energy is stronger in the dimers of the heavier elements in agreement with the MEP results. The ρr values at the bond CPs are indicated in italics close to them. They are also very similar in line with the interaction energies and equilibrium distances. The ρr value at the bond CP in **1 a** (Figure 4) is around trice the ρr value at the bond CP of the ReO_4^-···ReO_4^- dimer in water, thus revealing that the interaction is stronger in the solid state. Due to the effect of the water solvation, the distances of the optimized dimers are long, to minimize the electrostatic repulsion; they are longer than the sum of Ma and O van der Waals radii and much longer than in crystalline **1 a**,**b**. In order to consider entropic effects in water, we have also calculated the free energy values for the dimers represented in Figure 6. As expected, due to the unfavorable entropic effect, the ΔG values become positive, which are +9.5, +11.3 and +12.9 kcal/mol for the homodimers of MnO_4^-, TcO_4^- (b) and ReO_4^-, respectively. Therefore, despite the favourable enthalpic term, the existence of such interactions is not likely to occur in water solution unless a high concentration of the

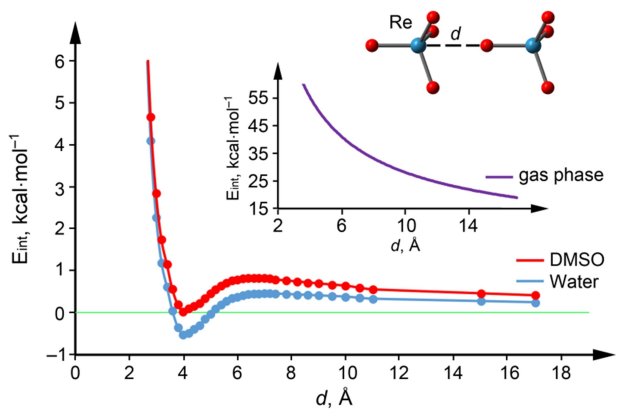

Figure 5. Energetic profiles obtained by varying the interatomic distance (d) in the ReO_4^-···ReO_4^- dimer at the PBE0-D3/def2-TZVP level of theory.

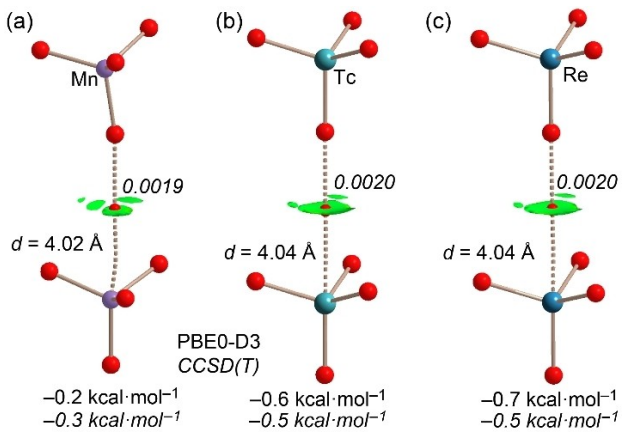

Figure 6. QTAIM distribution of intermolecular bond critical points (red spheres) and bond paths for the homodimers of MnO_4^- (a), TcO_4^- (b) and ReO_4^- (c) considering effects of water solvent. Electron density at bond CPs that characterize the MaBs are given in italics (a.u.). The superimposed NCIplot isosurface (RDG isovalue = 0.5 a.u.) is shown, The cut-off ρ = 0.04 a.u. has been used. Color range −0.035 a.u. ≤ (signλ_2) ρ ≤ 0.035. Level of theory: PBE0-D3/def2-TZVP and CCSD(T)/def2-TZVP.

MaO_4^- is used, as it has been demonstrated in saturated phosphate solutions.[25–27]

Several interactions can and do enable for the formation of anion···anion adducts by balancing the coulombic repulsion between charges with the same sign. The attractive force localized in the region of the HB between two protic hydroxyanions (e.g., HCO_3^-, HSO_4^-, and $H_2PO_4^-$) allows for the formation of dimers which can be stable in the gas, liquid, and solid phases.[25,28] Halogen bond formation explains the presence, in crystalline solids, of infinite chains formed on anions self-assembly.[29,30] The stability of anion···anion adducts given by polyatomic anions of elements of groups 2, 13, 15 and even 18 was rationalized resorting to the anisotropic distribution of the electron density in the anions and to the formation of alkaline earth metal bond,[31] triel bond,[32] pnictogen bond,[6,33] noble gas bond,[34] respectively. Importantly, the same approach has been employed to account for the formation of anion···anion adducts involving perhalometallates of d block elements, namely coinage bond[35] and spodium bond[36,37] explained the formation of anion···anion adducts involving elements of groups 11 and 12.

The combined experimental and theoretical investigation reported here provides strong evidence that interactions between electron rich atoms and the metal of tetroxide anions of group 7 elements are an additional case of attractive and σ-hole interactions robust enough to drive the formation of anion···anion adducts. The metal of one Mn/ReO_4^- unit acts as electron acceptor and the oxygen of another Mn/ReO_4^- unit, or the neutral oxygen of a nearby molecular entity, as the donor. The name matere bond (MaB) is proposed to categorize these noncovalent interactions, to signify the electrophilic role of the metal, and to differentiate these interaction from the classical metal-ligand coordination bond. DFT and *ab initio* calculations suggest that MaB driven anion···anion interactions involving MaO_4^- unit may exist also in solution at high concentrations.

Acknowledgements

A.F. acknowledges MICIU/AEI of Spain (CTQ2017-85821-R, FEDER funds) for financial support. Open Access Funding provided by Politecnico di Milano within the CRUI-CARE Agreement.

Conflict of Interest

The authors declare no conflict of interest.

Keywords: anion-anion interaction · group 7 · matere bond · noncovalent interaction · σ-hole

[1] P. Politzer, J. S. Murray, T. Clark, G. Resnati, *Phys. Chem. Chem. Phys.* **2017**, *19*, 32166–32178.
[2] G. Cavallo, P. Metrangolo, R. Milani, T. Pilati, A. Priimagi, G. Resnati, G. Terraneo, *Chem. Rev.* **2016**, *116*, 2478–2601.
[3] M. Fourmigué, A. Dhaka, *Coord. Chem. Rev.* **2020**, *403*, 213084.
[4] J. S. Murray, P. Lane, T. Clark, K. E. Riley, P. Politzer, *J. Mol. Model.* **2012**, *18*, 541–548.
[5] J. S. Murray, P. Politzer, *J. Comput. Chem.* **2017**, *39*, 464–471.
[6] A. Bauza, A. Frontera, T. J. Mooibroek, *Nat. Commun.* **2017**, *8*, 14522.
[7] T. Brinck, J. S. Murray, P. Politzer, *Int. J. Quantum Chem.* **1992**, *44*, 57–64.
[8] V. Amico, S. V. Meille, E. Corradi, M. T. Messina, G. Resnati, *J. Am. Chem. Soc.* **1998**, *120*, 8261–8262.
[9] A. Daolio, P. Scilabra, G. Terraneo, G. Resnati, *Coord. Chem. Rev.* **2020**, *413*, 213265.
[10] K. T. Mahmudov, A. V. Gurbanov, V. A. Aliyeva, G. Resnati, A. J. L. Pombeiro, *Coord. Chem. Rev.* **2020**, *418*, 213381.
[11] A. Bauzá, A. Frontera, *Coord. Chem. Rev.* **2020**, *404*, 213112.
[12] S. J. Grabowski, *Coord. Chem. Rev.* **2020**, *407*, 213171.
[13] G. Cavallo, P. Metrangolo, . Pilati, G. Resnati, G. Terraneo, *Cryst. Growth Des.* **2014**, *14*, 2697–2702.
[14] A. Daolio, A. Pizzi, M. Calabrese, G. Terraneo, S. Bordignon, A. Frontera, G. Resnati, *Angew. Chem. Int. Ed.* **2021**, *60*, 14385–14389.
[15] J. H. Stenlid, T. Brinck, *J. Am. Chem. Soc.* **2017**, *139*, 11012–11015.
[16] A. Bauzà, I. Alkorta, J. Elguero, T. J. Mooibroek, A. Frontera, *Angew. Chem. Int. Ed.* **2020**, *59*, 17482–17487; *Angew. Chem.* **2020**, *132*, 17635–17640.
[17] The term short, or close, contact is used to denote interactions shorter than the sum of van der Waals radii of involved atoms. For Mn, Re and O the used radii are 205, 205 and 155 pm, respectively (S. S. Batsanov, *Inorg. Mater.* **2001**, *37*, 871–885).
[18] The "normalized contact" (Nc) is the ratio between the observed Mn/Re···O distances and the sum of van der Waals radii. Nc is a useful indicator, allowing for a more rigorous comparison of separations among different short contacts than absolute values of interaction lengths. The primary sources of used van der Waals radii and a discussion of the reliability of their use are in Section S3.1.
[19] G. Resnati, P. Metrangolo, *Coord. Chem. Rev.* **2020**, *420*, 213409.
[20] L. Bian, H. Shi, X. Wang, K. Ling, H. Ma, M. Li, Z. Cheng, C. Ma, S. Cai, Q. Wu, N. G., X. Xu, Z. An, W. Huang, *J. Am. Chem. Soc.* **2018**, *140*, 10734–10739.
[21] R. M. Gomila, A. Bauzá, T. J. Mooibroek, A. Frontera, *CrystEngComm* **2021**, *23*, 3084–3093.
[22] P. Scilabra, G. Terraneo, A. Daolio, A. Baggioli, A. Famulari, C. Leroy, D. L. Bryce, G. Resnati, *Cryst. Growth Des.* **2020**, *20*, 916–922.
[23] B. Galmés, J. Adrover, G. Terraneo, A. Frontera, G. Resnati, *Phys. Chem. Chem. Phys.* **2020**, *22*, 12757–12765.
[24] E. D. Glendening, C. R. Landis, F. Weinhold, *WIREs Comput. Mol. Sci.* **2012**, *2*, 1–42.
[25] W. Zhao, A. H. Flood, N. G. White, *Chem. Soc. Rev.* **2020**, *49*, 7893–7906.
[26] C. W. Childs, *J. Phys. Chem.* **1969**, *73*, 2956–2960.
[27] R. H. Wood, R. F. Platford, *J. Solution Chem.* **1975**, *4*, 977–982.
[28] Ignasi Mata, Elies Molins, Ibon Alkorta, Enrique Espinosa, *J. Phys. Chem. A* **2015**, *119*, 183–194.
[29] J. M. Holthoff, E. Engelage, R. Weiss, S. M. Huber, *Angew. Chem. Int. Ed.* **2020**, *59*, 11150–11157; *Angew. Chem.* **2020**, *132*, 11244–11251.
[30] Y. Li, L. Meng, Y. Zeng, *ChemPlusChem* **2021**, *86*, 232–240.
[31] W. Zierkiewicz, R. Wysokiński, M. Michalczyk, S. Scheiner, *ChemPhysChem* **2020**, *21*, 870–877.
[32] R. Wysokiński, M. Michalczyk, W. Zierkiewicz, S. Scheiner, *Phys. Chem. Chem. Phys.* **2021**, *23*, 4818–4828.
[33] S. Scheiner, R. Wysokiński, M. Michalczyk, W. Zierkiewicz, *J. Phys. Chem. A* **2020**, *124*, 4998–5006.
[34] A. Grabarz, M. Michalczyk, W. Zierkiewicz, S. Scheiner, *Molecules* **2021**, *26*, 2116.
[35] A. Daolio, A. Pizzi, G. Terraneo, M. Ursini, A. Frontera, G. Resnati, *Angew. Chem. Int. Ed.* **2021**, *60*, 14385–14389.
[36] R. Wysokiński, W. Zierkiewicz, M. Michalczyk, S. Scheiner, *ChemPhysChem* **2020**, *21*, 1119–1125.
[37] R. Wysokiński, W. Zierkiewicz, M. Michalczyk, S. Scheiner, *ChemPhysChem* **2021**, *22*, 818–821.

Manuscript received: September 16, 2021
Accepted manuscript online: September 19, 2021
Version of record online: September 28, 2021